



Microscopic inhomogeneity induced thermal fluctuation in high temperature superconductors

D Behera^{1*}, R Biswal², U K Mohapatra² and N C Mishra¹

¹Department of Physics National Institute of Technology Rourkela 769 008 Orissa India

²Department of Physics Utkal University Bhubaneswar 751 004 Orissa India

E-mail dbehera@nitrkl.ac.in

Abstract Superconducting order parameter fluctuation (SCOPF) region in a set of pristine bulk sinter (YBCO) thick films and $\text{YBa}_2\text{Cu}_3\text{O}_{7-y}/\text{Ag}$ (YBCO/Ag), $\text{Y}_{1-x}\text{Ca}_x\text{Ba}_2\text{Cu}_3\text{O}_{7-y}/\text{Ag}$ composite samples are studied by varying the driving current in the first and Ag content in last two systems. The mesoscopic inhomogeneities that influence the tailing region arises due to most of Ag residing at the grain boundaries in the composites or due to current induced suppression of Josephson tunnelling of supercurrent across grain boundaries. These inhomogeneities in principle should not influence the SCOPF region. Ca doping at yttrium site in the grains of YBCO directly influences the SCOPF region. We observe a strong variation of T_{1D} with Ag and associated increase in coupling strength. It is observed that SCOPF region is more affected in Ca doped sample as compared to Ag composite one. The SCOPF being basically a precursor to the onset of superconductivity in the grains, our results thus show that the SCOPF is affected due to either Ag diffusing into the grains in the composites or due to Ca occupying Y site in the doped samples.

Keywords Superconductors, order parameter fluctuation, charge fluctuation

PACS Nos. 74.62.Dh, 74.72.Bk, 74.81.Bd

1. Introduction

Superconducting and normal state properties in $\text{YBa}_2\text{Cu}_3\text{O}_{7-y}$ (YBCO) system is controlled by charge carriers. Carrier density can be enhanced either by increase of oxygen content or by on-site cationic substitutions with dopants of lower valence state. Ca doping at Y site has created much interest in the scientific community as this doping turns an oxygen-deficient YBCO system from insulator to superconductor. On the other hand, Ca doping tends to decrease the oxygen content in YBCO resulting in the reduction of transition temperature T_c [1,2]. This decrease of oxygen content is countered by extra holes introduced by Ca^{2+} ions [3,4]. In addition to affecting T_c , Ca doping decreases normal

state resistivity, increases critical current J_c , affects the interlayer coupling strength J [5] and hence influences the superconducting order parameter fluctuation (SCOPF) [6] region above T_c . Not just the electrical properties even the structure changes from orthorhombic to tetragonal [7] and grain size reduces [8] on Ca doping

Unlike Ca, which occupies lattice in the grains, Ag is preferentially disposed at the grain boundaries and forms composites with YBCO. Remaining at the grain boundary it reduces weak link between the grains, enhances J_c reduces normal state resistivity [9] without affecting T_c . Though most of the studies [10,11] point to the disposition of Ag at the grain boundaries, some of the studies [12] have indicated that some amount of Ag goes into the grains. The conflict that whether Ag remains only at the grain boundaries and brings in microstructural dependent modifications and brings in associated modifications, is still not resolved.

The nature of the superconducting transition, particularly the region just above and below T_c are strongly influenced by the intra and intergranular characteristics respectively. The SCOPE region above T_c is an indicator of the onset of fluctuating superconducting state inside the grains. The SCOPF is much enhanced in high T_c superconductor like YBCO as compared to the low T_c ones due to very short coherence length ξ_c , relatively low penetration depth, λ and high transition temperature, T_c . Thus, as the sample temperature is lowered from room temperature towards T_c , the fluctuating Cooper pairs begin to be created spontaneously from a temperature well above T_c , the number of Cooper pairs increases rapidly at the expense of the normal electron density. As a result the net resistance of the sample decreases, which is known as the fluctuation induced excess conductivity or paraconductivity.

The paracoherent phase in the transition region becomes fully coherent below T_c with zero resistivity or infinite conductivity at a temperature, T_{∞} . The region between T_c and T_{∞} is controlled by percolation process through the inter-granular weak links, which is accompanied by thermal fluctuations [3, 13]. For decreasing temperature, phase coupling between the grains takes place and gradually a paracoherent-coherent transition characteristics of a granular superconductor, occurs. The zero-resistance at the temperature T_{∞} , characterizes the onset of global superconductivity in the samples where the longrange superconducting order is achieved. The approach to this state in the form of tailing indicates that the Josephson tunnelling across the grain boundary weak links progressively couple the superconducting grains to each other. This type of tailing feature in the resistive transition close to T_{c0} has been seen mostly in granular superconductors. In the tailing region close to T_{c0} , this heterogeneous medium consists of two components. For the first component we consider the superconducting grains and the grain boundary weak links through which superconductivity is established through Josephson tunneling. The second component consists of weak links which are not superconducting, either due to the link being too weak or due to the measuring current exceeding the J_c of the corresponding link or the temperature being higher than the T_c of that link. For $T < T_{\infty}$, the first component provides the channel for the transport of supercurrent. For $T_{\infty} < T < T_c$, the volume of the

first component is not adequate enough to provide a percolative path for super current and the $R-T$ transition shows a tail with $R \neq 0$. Only when $T \leq T_{c0}$, a percolative path through the first component is established and a global superconductivity is established in the sample with R going to zero.

A large number of studies have indicated the influence of the inter-granular characteristics like weak links and secondary phases at the grain boundaries on the SCOPF region [14-16]. The SCOPF being basically a consequence of the onset of superconductivity in the grains, the influence of the secondary phases at the grain boundaries on the SCOPF region is still a mystery. In the present study, we examine the tailing region below T_c and the SCOPF region and T_c by increasing current in a set of pure YBCO thick films and with varying Ag content in a set of YBCO/Ag thick film and $Y_{1-x}Ca_x-123/Ag$ bulk sample. A comparison of the influence of these two control parameters (current and Ag content) on both the regions (tailing and the SCOPF) indicates that a fraction of Ag diffuses into the grains of YBCO/Ag composite thick films.

2 Experiment

$Y_{1-x}Ca_xBa_2Cu_3O_{7-y}(Y_{0.9}Ca_{0.1}-123)$ was prepared from the stoichiometric amount of Y_2O_3 , $BaCO_3$, $CaCO_3$ and CuO through standard solid state reaction. For the preparation of $(Y_{1-x}Ca_x-123)/Ag$ composite bulk sinters, Ag_2O was mixed with $Y_{0.9}Ca_{0.1}-123$ powder before the final stage of sintering. The samples were pressed into pellets, annealed at $920^\circ C$ for 12 hrs and cooled to $400^\circ C$ where they stayed for 12 hrs with oxygen flowing. Then the samples cooled to room temperature at a rate of $2^\circ C/min$.

Thick films of $YBa_2Cu_3O_{7-y}/Ag$ composites were prepared by diffusion reaction technique. Y_2BaCuO_5 (Y211), the insulating green phase of YBCO was used as the substrate. The diffusion reaction method involved the reaction of the substrate (Y211) with an over-layer of $Ba_3Cu_5O_8$ (deposited by doctor blading) at $920^\circ C$ in ambient atmospheric condition leading to the formation of YBCO film of about $10 \mu m$ thick.

The temperature dependent resistance, $R(T)$ was measured using four-probe technique with a Nanovoltmeter (Keithley-181) and an indigenously developed constant current source. With the voltage resolution of $10^{-7} V$ of the Nanovoltmeter, a constant current of 1 mA flowing through the samples gives a resolution $\sim 1 \mu \Omega$ in the measured resistance. A Closed Cycle Helium Refrigerator (APD cryogenics-HC2) and a Temperature Controller (Scientific Co 9600-1) were used for temperature variation. The Temperature Controller used a Si diode sensor having a temperature resolution of $\pm 0.1 K$. A computer controlled data acquisition system was used to acquire the resistance data from 40 K to room temperature. Resistance data were acquired during the heating cycle with heating rate confined to 3 K per minute.

To study the current dependence of the superconducting transition, we passed 100 μA -25 mA DC current through the two outer probes of the four-probe arrangement by

current pulse technique. The Voltage developed across the two inner probes was measured by the nanovoltmeter. Pulsing of current was necessary to avoid sample heating and damage to the contacts.

3. Results and discussion

Figure 1 shows the temperature dependence of normalized resistance, $R_n(T)$ measured at different driving current through a pure YBCO thick film. The resistance was normalized with respect to the value obtained at 100K. As shown in this figure, onset of superconductivity occurs at a temperature, T_{ci} where R_n shows a sharp decrease. This is the temperature where superconductivity sets in the grains with grain boundaries still remaining normal. At a lower temperature, T_{cj} , $R_n(T)$ for different currents starts to branch out. The branching of $R_n(T)$ indicates the beginning of the non-ohmic behaviour of the weak links below T_{cj} from the ohmic behaviour above T_{cj} . This temperature, therefore characterizes the establishment of superconductivity across some of the grain boundaries (strongly linked ones) due to Josephson tunnelling. As the temperature is further decreased the resistance vanishes at T_{co} where global superconductivity prevails.

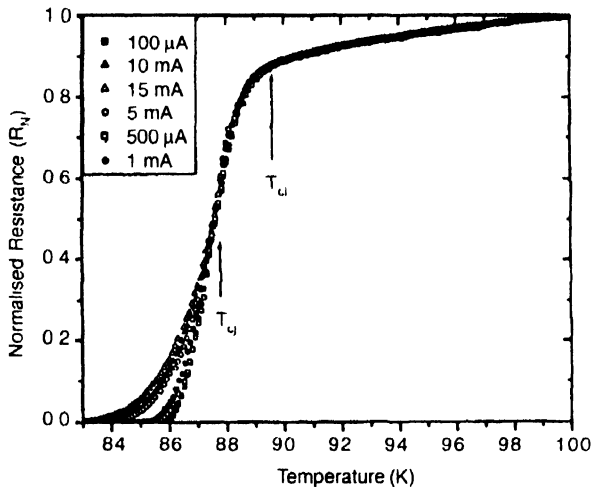


Figure 1. Temperature dependence of normalized resistance, R_n at different driving currents in pure YBCO thick film

With increasing current, tailing below T_{cj} becomes more pronounced and the T_{cc} progressively shifts to lower values. The T_{ci} and T_{cj} however remain unaffected at all currents up to 20mA. Not just these transition temperatures, even the mean field region where thermal fluctuation leads to the excess conductivity above T_{ci} is also not affected. The T_{ci} and T_{cj} and the SCOPF region not depending on the driving current through the sample clearly indicates that the superconductivity in the grains is not affected. On the other hand T_{co} shifting to lower temperature side with increasing current clearly indicates that some of the inter-granular junctions are driven from the non-dissipative to the dissipative state driving them from the Josephson coupled state to the normal state.

Figure 2 shows the temperature variation of the normalized resistance, (also normalized with respect to the resistance at 100 K) in a set of YBCO/Ag composite thick films with varying Ag concentration. The YBCO/Ag composite thick films represent a class of granular superconductor where the charge transport occurs in an interpenetrating superconducting and normal state percolative medium. In YBCO/Ag composites, it is believed that Ag resides at the grain boundaries and modifies the microstructure of the sample to a large extent. With increasing Ag concentration in the sample T_{c0} shifts to lower temperature side. The observed decrease of T_{c0} (Figure 2) is therefore of consequence of the progressive decoupling of the superconducting grains with increasing Ag content at the grain boundaries in the films.

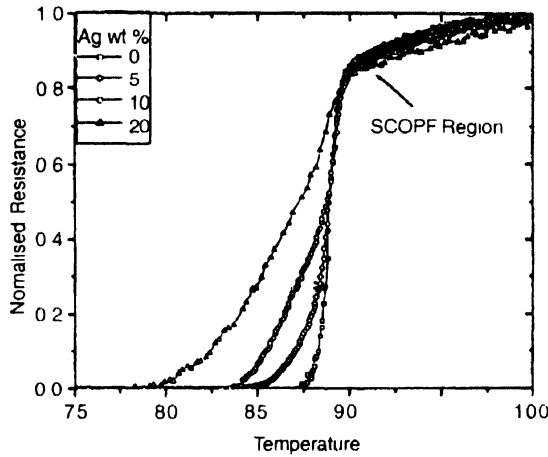


Figure 2. Temperature dependence of normalized resistance, R_n at different Ag content in YBCO/Ag composite thick films

The temperature dependent electrical resistance (R vs T) of $Y_{0.9}Ca_{0.1}-123$ and $Y_{0.9}Ca_{0.1}-123/Ag$ (10 wt.%) are shown in the Figure 3. Though the superconducting transition occurs

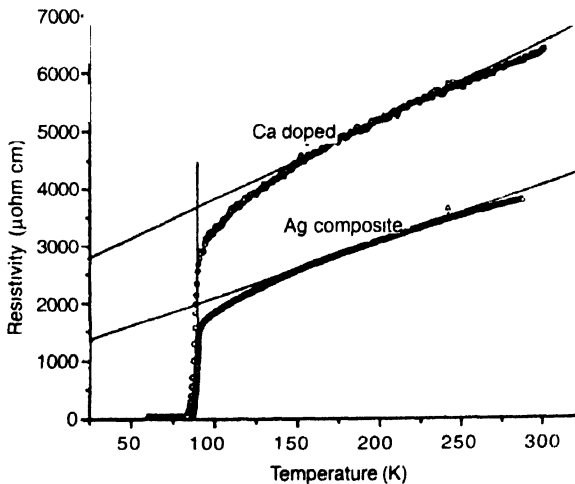


Figure 3. Temperature dependent resistivity in $Y_{1-x}Ca_xBa_2Cu_3O_{7-y}$ ($x = 0.1$) and $Y_{1-x}Ca_xBa_2Cu_3O_{7-y}/Ag$ (Ag 10 wt.%) sample.

at same temperature in both the systems, Ag composite one shows higher T_{c0} . Addition of Ag in the system thus does not degrade the transition temperature rather improves the coupling strength and enhances the microstructural modifications [13]. The SCOPF region however is affected in Ca doped sample as compared to Ag composite one (Figure 3)

The similarity of shifting of T_{c0} in Figure 1 and Figure 2, in response to different control parameters : variation of current in YBCO thick films and variation of Ag contents in YBCO/Ag composite thick films respectively point to a single phenomenon in the granular superconductor. That is, both the increased current and increased Ag content suppress the Josephson coupling across the grain boundaries. Thus both influence the inter-granular characteristics of the sintered granular superconductors as is used in the present study. In principle, the grain boundary modification either due to increased current or increased Ag content should not affect the grains, which is characterized by T_{cI} , T_{cI} and SCOPF region. In fact we find that the current does not affect these parameters in pure YBCO sample. In YBCO/Ag composite thick films however, Ag content in the samples influences both the inter-as well as the intra-granular regions significantly. In addition to the T_{cI} shifting to lower temperatures as in the case of higher current, the T_{cI} and the SCOPF regions are affected with increasing Ag content. This indicates that Ag not only influences the grain boundary characteristics, it also influences the grains themselves.

The mesoscopic inhomogeneities like grain boundaries, crack, voids *etc.* having much larger length scale than the superconducting coherence length, ξ and being temperature independent are not expected to influence the SCOPF region [1]. These inhomogeneities dominate the region describing the approach to the zero resistance state. The microscopic inhomogeneities such as structural (twin boundaries, stacking faults) and chemical imperfections (oxygen deficiencies *etc.*) inside the grains occur in a length scale smaller than the mesoscopic inhomogeneities, but still larger than ξ . These inhomogeneities therefore have negligible effect on the SCOPF region [1]. Many studies however have shown that the inhomogeneities crucially influence both the critical and the mean field region of SCOPF, particularly the excess conductivity and its divergence as T_c is approached from high temperature side [14-16]. Cukauskas *et al* [14] for example have shown expansion of the critical region with increasing secondary phases associated with reduced value of the critical exponent. Similar observation has been made by Aswal *et al* [15] who have also shown that increased secondary phases at the grain boundaries leads to the appearance of both static and dynamic critical region. The exponents in the mean field region as well as the Lawrence-Doniach crossover temperature, T_{LD} characterising the transition from 2 to 3 dimensional nature of SCOPF have all been affected by such inhomogeneities [17]. In the background of such conflicting analysis of the influence of inhomogeneities on the SCOPF region, we show that the SCOPF remains unaffected if the grain boundaries are driven to normal state simply by increasing current, while having second phases like Ag in the sample influences the SCOPF region dramatically.

For the analysis of the fluctuation effect, we have used the Aslamazov and Larkin (AL) [18] phenomenological relation between the excess conductivity and the reduced temperature as

$$\Delta\sigma = A\epsilon^{-\lambda} \tag{1}$$

where $\epsilon = (T - T_c)/T_c$, the reduced temperature defined with respect to T_c . The excess conductivity, $\Delta\sigma$ was obtained by subtracting the normal conductivity, $\sigma_n(T)$ from the measured conductivity, $\sigma(T)$ in a temperature interval close to T_c . The $\sigma_n = 1/\rho_n$ was obtained by linear fitting of the resistivity curve in a temperature interval 250 to 150 K and extrapolating the same to temperatures below T_c . The AL relation is based on the Ginzburg-Landau (GL) mean field theory and is valid only in a mean field temperature $\sim 1.01 T_c$ to $1.1 T_c$. The amplitude A is a temperature independent parameter and its value for 2D and 3D cases is $e^2/16\hbar d$ and $e^2/32 \xi_c(0)$ respectively, where d and $\xi_c(0)$ are the effective layer spacing and the GL correlation length respectively.

Approaching the superconducting transition temperature from above, the fluctuations exhibit filamentary nature corresponding to one dimension, or planar fluctuation corresponding to 2- dimensions or fluctuation in all 3- dimensions. From $\rho - T$ plot different regions are also identified. The crossover temperature between different regions is assigned such as T_{LD} (2D to 3D) and T_G (3D to critical). Lawrence and Doniach (LD) [19] extended AL model for layer superconductors where conduction occurs mainly in 2D planes, which are coupled via Josephson tunnelling. Assuming $\xi_a(0) = \xi_b(0)$, the excess conductivity parallel to layers in the LD model is

$$\Delta\sigma = \left(e^2/16\hbar d \epsilon \right) \left[1 + B_{LD} \epsilon^{-1} \right]^{-1/2} \tag{2}$$

where the LD parameter $B_{LD} = [2\xi_c(0)/d]^2$. This expression predicts a crossover from 2D to 3D behaviour of the order parameter fluctuations in the mean field region at temperature

$$T_{LD} = T_c \left\{ 1 + [2\xi_c(0)/d]^2 \right\}. \tag{3}$$

We have used the LD theory to extract T_{LD} (figure 3) from which the coupling strength between superconducting layers given by $J = [\xi_c(0)/d]^2$ was obtained.

Different regions of the SCOPF analysed as above in Ag composite samples are shown in Figure 4. From the variation of the different crossover temperatures from one region of SCOPF to another region, it is observed that T_c almost remains unaffected (Figure 2), whereas T_{LD} and T_G show a significant increase with increasing Ag content (Figure 4). The decrease of T_{c0} (Figure 2) reflects the Ag induced mesoscopic modification in the grains, which also explains the widening of the critical region associated with increase in T_G . The strong variation of T_{LD} with Ag content associated with increase of the interplanar coupling strength J . Figure 5 shows the effect of Ca in decreasing T_c and increasing T_{LD} .

Further when Ag made as a composite to the system containing Ca, both T_c and T_{LD} increases. The crossover temperature between 2D-3D region T_{LD} is shifted towards higher temperature side. Ca doping at the Y site is expected to affect the SCOPF parameters as it basically affect the intragrain behaviour. Hence it can be inferred that some amount of Ag goes to lattice site. Since microscopic inhomogeneity has been shown to have an insignificant effect on the SCOPF [1], we explain the strong dependence of T_{LD} on Ag by involving its role in modifying the overall electronic structure of grains [20].

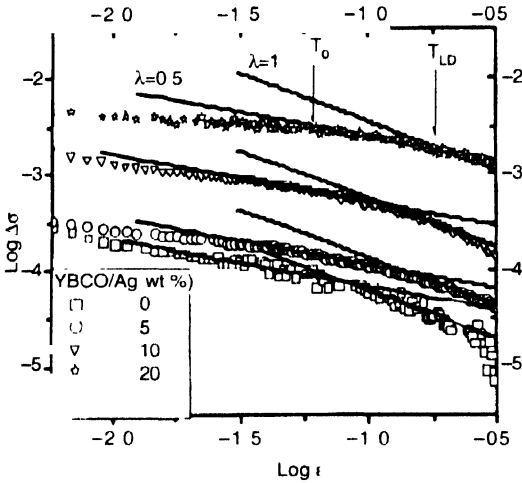


Figure 4. Log – Log plots of excess conductivity as a function of reduced temperature for YBCO/Ag composite thick films for different Ag content.

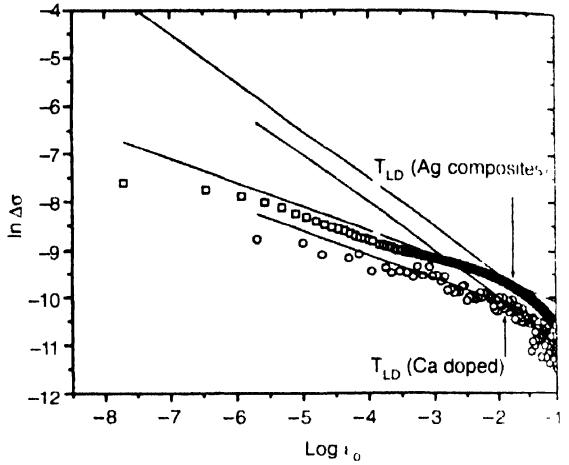


Figure 5. Log – Log plots of excess conductivity as a function of reduced temperature for $Y_{1-x}Ca_xBa_2Cu_3O_{7-y}$ ($x = 0.1$) and $Y_{1-x}Ca_xBa_2Cu_3O_{7-y}/Ag$ composite thick films with Ag 10 wt %

4. Conclusion

Our study of the temperature dependence of resistivity in YBCO/Ag composite thick films with varying Ag content and $Y_{1-x}Ca_xBa_2Cu_3O_{7-y}/Ag$ have revealed that a fraction of the Ag diffuse into the grains. The intra-granular features like the SCOPF region and the onset of superconductivity are thus significantly modified with Ag concentration in the films. This observation is further supported by our study on pure YBCO thick films where the current dependence of the $R_n(T)$ only influences the intergranular characteristics and leaves the granular characteristics unaffected.

Table 1. Ag content dependence of different transition temperatures (zero resistive, mean field, Ginzburg and Lawrence-Doniach) and the inter-planar coupling strength of YBCO / Ag composite thick films.

wt.% of Ag	$T_{c0}(K)$	$T_c(K)$	crossover temperatures (K)		$J(10^{-2})$
			T_G	T_{LD}	
0	87.2 ± 0.4	88.9 ± 0.2	90.6 ± 0.8	96.9 ± 0.2	2 ± 0.12
5	83.4 ± 1.5	89.0 ± 0.2	92.2 ± 1.5	100.5 ± 0.2	3 ± 0.12
10	83.0 ± 1.0	89.2 ± 0.2	92.3 ± 0.5	99.2 ± 0.2	3 ± 0.12
20	80.5 ± 2.0	88.6 ± 0.2	96.0 ± 1.4	106.4 ± 0.2	5 ± 0.12

References

- [1] J Maza and F Vidal *Phys. Rev* **B43** 10560 (1991)
- [2] Z H Wang *Mod. Phys. Lett* **B10** 1027 (1996)
- [3] P Pureur, C R Menegotto, P Rodrigues, J Schaf and J V Kunzler *Phys Rev* **B47** 11420 (1993)
- [4] D Behera, S K Dash and N C Mishra *Indian J Phys* **77A** 133 (2003)
- [5] D Behera, Y K Mohapatra and N C Mishra *Indian J Phys* **78(8)** 803 (2004)
- [6] U K Mohapatra, R Biswal, D Behera and N C Mishra *Supercond Sci Technol* **19** 335 (2006)
- [7] A K Gosh, S K Bandyopadhyay, P Barat, Pintu Sen and A N Basu *Physica* **C264** 255 (1996)
- [8] A Schmehl, B Goetz, R R Schulz, C W Schneider, H Viefelfeldt, H Hilgenkamp and J Mannhart *Eur Phys Lett.* **47** 110 (1999)
- [9] J T Kucera and J C Bravman *Phys. Rev.* **B51** 8582 (1995)
- [10] R Rangel, D H Galvan, G A Hiratar, E Adem, F Morales and M B Maple *Supercond Sci Technol* **12** 264 (1999)
- [11] Ch Chang and Y Zhao *J Appl Phys* **93** 2292 (2003)
- [12] Ch Zhang, A Kulpa and A C D Chaklader *Physica C* **252** 67 (1995)
- [13] V N Viera, P Pureur and J Schaf *Physica* **C353** 241 (2001)
- [14] E J Cukauskas and L H Allen *J Appl. Phys* **84** 6187 (1998)
- [15] D K Aswal, A Singh, S Sen, M Kaur, C S Viswandham, G L Goswami and S K Gupta *J Phys and Chem of Solids* **63** 1797 (2002)
- [16] T Sato, H Hakane, S Yamazaki and N Mori *Physica* **C372** 1208 (2002)
- [17] A S Sidorenko, V I Zdravkov, V V Ryazanov, M Klemm, S Horn, R Tideeks, C Muller and A Wixforth *J Supercond* **17** 211 (2004)
- [18] L G Aslamazov and A I Larkin *Sov Phys. Solid State* **10** 875 (1968)
- [19] W E Lawrence and S Doniach *Proceeding of Twelfth International Conference on Low Temperature Physics, Kyoto*, p361 (1970)
- [20] H P Mohapatra, D Behera, S Misra, N C Mishra and K Patnaik *J Superconductivity* **6** 359 (1993)